

Structural analysis and magnetic properties of the 1D $[\text{Fe}(\text{dca})_2\text{bipy}(\text{H}_2\text{O})]\cdot 1/2\text{H}_2\text{O}$ and the 3D $[\text{Ni}(\text{dca})_2\text{bipy}]$ (dca = dicyanamide; bipy = 4,4'-bipyridine)

Susana Martín,^a M. Gotzone Barandika,^a J. M. Ezpeleta,^b Roberto Cortés,^a J. I. Ruiz de Larramendi,^{*a} Luis Lezama^c and Teófilo Rojo^{*c}

^a Departamento de Química Inorgánica, Facultad de Farmacia, Universidad del País Vasco, Apdo. 450, Vitoria 01080, Spain

^b Departamento de Física Aplicada, Facultad de Farmacia, Universidad del País Vasco, Apdo. 450, Vitoria 01080, Spain

^c Departamento de Química Inorgánica, Facultad de Ciencias, Universidad del País Vasco, Apdo. 644, Bilbao 48080, Spain. E-mail: qiproapt@lg.ehu.es

Received 24th June 2002, Accepted 3rd October 2002

First published as an Advance Article on the web 25th October 2002

The combined use of bipy (4,4'-bipyridine) and dca (dicyanamide) has led to the preparation of two polymeric compounds of formulae $[\text{Fe}(\text{dca})_2\text{bipy}(\text{H}_2\text{O})]\cdot 1/2\text{H}_2\text{O}$ (**1**) and $[\text{Ni}(\text{dca})_2\text{bipy}]$ (**2**). Both have been synthesised and characterised through IR and UV-Vis spectroscopies, thermal analysis, X-ray diffraction and measurements of the molar magnetic susceptibility. Compound **1** is 1D and exhibits weak antiferromagnetic interactions. Compound **2** consists of two interpenetrated 3D networks giving rise to weak ferromagnetic interactions. The formation of both types of structure can be related to the different Pearson acidities of Fe^{II} and Ni^{II} ions.

Introduction

The design of multidimensional networks has been an important area of research in coordination chemistry. Coordination polymers have been extensively reported exhibiting different combinations of metallic cations, dipyriddy-type organic ligands and pseudohalide ligands. In this sense, the ligand dicyanamide (dca) has been widely confirmed to be a good candidate for the preparation of extended networks in coordination chemistry.¹ This pseudohalide ligand exhibits several coordination modes that account for its high versatility in the formation of intermetallic connections. Thus, besides the monodentate terminal coordination,² bi-,³ tri-⁴ and even tetra-dentate⁵ modes have been reported for dca (Chart 1).

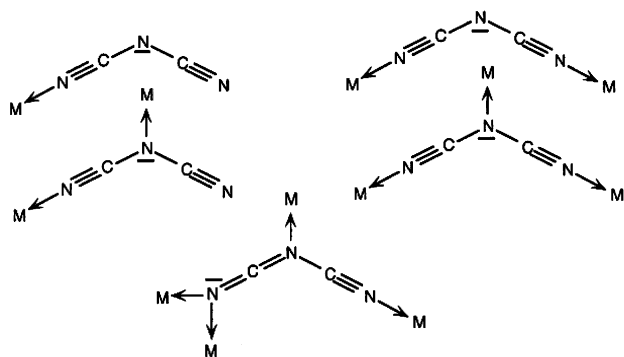


Chart 1

In this context, we have already reported on several M-dca-bpm compounds (M = Mn, Co, Ni, Cu, Zn and bpm = 2,2'-bipyrimidine).⁶ The isomorphous compounds $[\text{M}_2(\text{dca})_4\text{bpm}]$ (M = Mn, Cu, Zn) exhibit ladder-like structural units connected through single dca bridges giving rise to 3D networks. A second structural arrangement has been found for the Ni and Co⁷

compounds of formula $[\text{M}_2(\text{dca})_4\text{bpm}]\cdot \text{H}_2\text{O}$. These coordination polymers also exhibit ladder-like structural units but their connections result in 2D networks. Additionally, it is worth mentioning that we have characterised another structural arrangement for Mn^{II} with dca and bpm. Thus, the compound $[\text{Mn}(\text{dca})_2\text{bpm}]$ shows a 1D structural array based on intermetallic connections through double dca bridges.^{6a}

The cited examples are illustrative of the relevance of the nature of the metallic cations in the structural features of the compounds. In this sense, we have been investigating the combination of the ligands dca and bipy (4,4'-bipyridine) with several divalent metallic cations. The ligand bipy has also been used for the preparation of extended frameworks⁸ as this dipyriddy-type ligand enhances the formation of intermetallic connections due to the relative 4,4'-position of the donor N-atoms.

This paper reports on the synthesis and magnetostructural characterisation of two M-dca-bipy compounds: $[\text{Fe}(\text{dca})_2\text{bipy}(\text{H}_2\text{O})]\cdot 1/2\text{H}_2\text{O}$ (**1**) and $[\text{Ni}(\text{dca})_2\text{bipy}]$ (**2**). Additionally, the influence of the nature of the metallic cation on the structural features of compounds **1** and **2** and other related compounds will be discussed on the basis of Pearson acidity criteria.

Experimental

Synthesis and chemical analysis

Synthesis of compound **1** was carried out by mixing an aqueous solution of $\text{FeCl}_2\cdot 4\text{H}_2\text{O}$ (0.50 mmol, 15 ml) and an aqueous solution of dca (1 mmol, 5 ml). Afterwards a methanolic solution of bipy (0.5 mmol, 15 ml) was added under continuous stirring. The resulting solution was filtered and left to stand at 2 °C. After several days, prismatic, red, X-ray quality single crystals were obtained (41% yield based on the metallic cation).

Synthesis of compound **2** was carried out similarly by using $\text{Ni}(\text{NO}_3)_2\cdot 6\text{H}_2\text{O}$. After several days, blue, poor-quality crystals

were obtained (45% yield based on the metallic cation). Further attempts to obtain good-quality crystals were unsuccessful.

Elemental analysis and atomic absorption results were in good agreement with the $\text{FeC}_{14}\text{H}_{11}\text{N}_8\text{O}_{1.5}$ stoichiometry for **1** and the $\text{NiC}_{14}\text{H}_8\text{N}_8$ stoichiometry for **2**. Found (calc. %): Fe, 14.99 (15.05); C, 44.72 (45.31); N, 29.84 (30.19); H, 3.10 (2.99) for **1**; Ni, 16.51 (16.92); C, 46.92 (48.46); N, 30.85 (32.30); H, 2.06 (2.32) for **2**.

Thermal analysis

TG curves were recorded for compounds **1** and **2** in the 25–500 °C temperature range. Compound **1** decomposes in two steps starting at 100 °C. The first of them finishing at 220 °C (93.8% of the initial mass found) can be attributed to the loss of 3/2 molecules of water per formula unit (loss of mass: 6.2% found, 6.45% calculated). The second step is an abrupt loss of 75.1% of the initial mass finishing at 315 °C (18.7% of the initial mass found) that should correspond to the pyrolysis of the dehydrated compound. Identification of the final residue for **1** through X-ray diffraction was not possible due to the low crystallinity of the samples. Thermal decomposition for **2** starts at 200 °C and finishes at 400 °C. In a first step (up to 335 °C), a loss of mass of 39.9% has been found that can be attributed to the pyrolysis of the bipy ligands (38.1% calculated). The second step corresponds to a loss of 37.4% of the initial mass that leads to the final residue (22.7% of the initial mass found). As for **1**, the residue for **2** has not been identified through X-ray diffraction.

Physical measurements

Microanalyses were performed with a LECO CHNS-932 analyser. Analytical measurements were carried out in an ARL 3410 + ICP instrument with Minitorch equipment. IR spectroscopy was performed on a Nicolet 520 FTIR spectrophotometer in the 400–4000 cm^{-1} region. Thermogravimetric analyses were carried out using a TA-Instruments SDT-2960 DSC-TGA unit at a heating rate of 5 °C min^{-1} in argon. Magnetic susceptibilities of powdered samples were carried out in the temperature range 5–300 K at values of magnetic field up to 10000 G, using a Quantum Design Squid magnetometer, equipped with a helium continuous-flow cryostat. The experimental susceptibilities were corrected for the diamagnetism of the constituent atoms (Pascal tables).

Crystal structure determination

Single-crystal X-ray measurements for compound **1** were taken at room temperature on an Enraf-Nonius CAD-4 diffractometer with graphite-monochromated Mo-K α radiation ($\lambda = 0.71070$ Å), operating in the $\omega/2\theta$ scanning mode using suitable crystals for data collection. Accurate lattice parameters were determined from least-squares refinement of 25 well-centred reflections. Intensity data were collected in the θ range 1–30°. During data collection, two standard reflections periodically observed showed no significant variation. Corrections for Lorentz and polarisation factors were applied to the intensity values.

The structure was solved by direct methods using the program SIR97⁹ and refined by a full-matrix least-squares procedure on F^2 using SHELXL97.¹⁰ Non-hydrogen atomic scattering factors were taken from *International Tables for X-Ray Crystallography*.¹¹ Crystallographic data and processing parameters for **1** are shown in Table 1.

It is worth mentioning that the structure for **1** shows remarkable disorder affecting the molecules of H₂O and the dca groups. Thus, the position of the oxygen atom corresponding to the coordination molecules of water has been split into two (O11 and O12, with occupation factors of 0.5) for a better structural resolution. Similarly, the position of the N6 central

Table 1 Crystal data and structure refinement for compound **1**

Formula	$\text{FeC}_{14}\text{H}_{11}\text{N}_8\text{O}_{1.5}$
<i>M</i>	371.16
<i>T</i> /K	293(2)
Crystal system	Tetragonal
Space group	$I4_1cd$
<i>a</i> /Å	22.366(5)
<i>c</i> /Å	13.311(2)
<i>U</i> /Å ³	6658(2)
<i>Z</i>	16
λ /Å ^a	0.71073
μ /mm ⁻¹	0.928
Unique data	3143
Observed data	3143
<i>R</i> (<i>R'</i>) ^b	0.0458 (0.1086)

^a Mo-K α radiation, graphite monochromator. ^b $R = [\sum||F_o| - |F_c||/\sum|F_o|]$, $R' = [\sum[w(F_o^2 - F_c^2)^2]/\sum[w(F_o^2)^2]]^{1/2}$ where $w = 1/\sigma^2(|F_o|)$.

Table 2 Structural data and refinement for compound **2**

Formula	$\text{NiC}_{14}\text{H}_8\text{N}_8$
<i>M</i>	346.97
<i>T</i> /K	298
Crystal system	Orthorhombic
Space group	$Pnma$
<i>a</i> /Å	16.576(8)
<i>b</i> /Å	11.773(7)
<i>c</i> /Å	8.478(3)
<i>U</i> /Å ³	1654(2)
<i>Z</i>	4
λ /Å	1.54056/1.54433
<i>R</i> _p ^a	6.81
<i>R</i> _p ^b	19.4
<i>R</i> _{wp} ^c	24.9

^a $R_b = 100[\sum|I_o - I_c|/\sum I_o]$; ^b $R_p = 100[\sum|y_o - y_c|/\sum y_o]$; ^c $R_{wp} = [\sum[w|y_o - y_c|^2]/\sum[w|y_o|^2]]^{1/2}$ where $w = 1/\sigma^2(|F_o|)$.

nitrogen atom of one of the dca groups has been split into two: N61 and N62, with occupation factors of 0.5. Additionally, an occupation factor of 0.5 has been assigned to the position of the oxygen atom corresponding to the crystallisation molecules of water (O2).

CCDC reference number 184701.

See <http://www.rsc.org/suppdata/dt/b2/b206069h/> for crystallographic data in CIF or other electronic format.

X-Ray powder diffraction data for compound **2** were collected on a PHILIPS X'PERT powder diffractometer with Cu-K α radiation in steps of 0.02° over the 5–60° 2θ -angular range and a fixed-time counting of 4 s at 25 °C. The powder diffraction patterns were indexed with the FULLPROF¹² program based on the Rietveld method¹³ using the *Profile Matching* option. Structural data for the isomorphous compound [Co(dca)₂bipy] (**3**)¹⁴ ($Pnma$, $a = 16.9221(7)$, $b = 11.4251(4)$, $c = 8.6147(3)$ Å) were used as initial data for the refinement of **2**. Crystallographic data and processing parameters for **2** are given in Table 2.

Results and discussion

Structural analysis

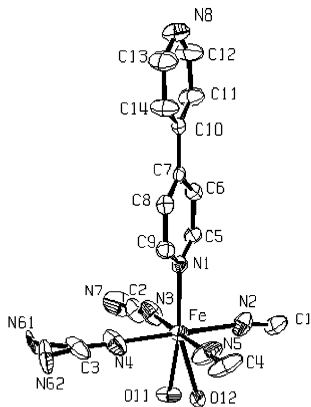
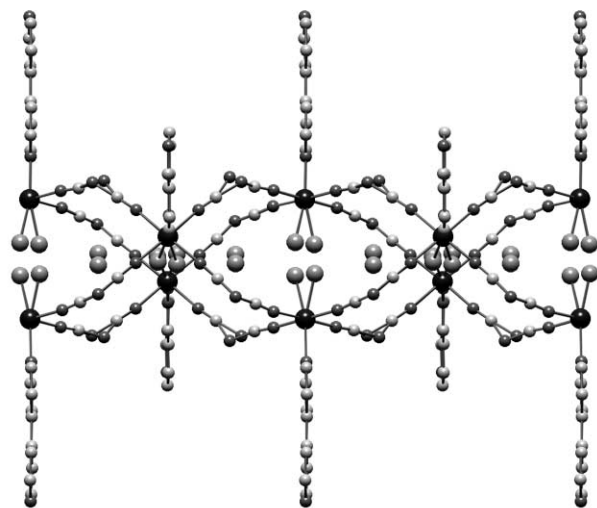
The structure for the 1D compound **1** consists of chains extending along the [001] direction. As seen in Fig. 1, each Fe metallic atom is octahedrally coordinated to five N atoms (four μ -1,5-dca groups on the equatorial sites and a terminal bipy ligand on one of the axial positions) and one O atom belonging to a molecule of water on the remaining axial position.

This way, as seen in Fig. 2, each Fe atom is connected to another four through μ -1,5-dca bridges. The structure for **1** also shows crystallisation molecules of water located on the cavities generated by the dca groups.

Table 3 Selected bond distances (Å) and angles (°) for compound **1**

Fe–N(1)	2.191(4)	Fe–N(5)	2.139(9)
Fe–N(2)	2.152(9)	Fe–O(11)	2.18(2)
Fe–N(3)	2.164(8)	Fe–O(12)	2.25(2)
Fe–N(4)	2.148(9)		
N(2)–Fe–N(1)	87.7(3)	N(4)–Fe–N(2)	179.0(4)
N(3)–Fe–N(1)	86.9(3)	O(11)–Fe–N(1)	166.4(6)
N(4)–Fe–N(1)	92.4(3)	O(12)–Fe–N(1)	164.2(6)
N(5)–Fe–N(1)	91.1(3)		

O11 and O12 atoms (with occupation factors of 0.5) correspond to the coordination molecule of water.

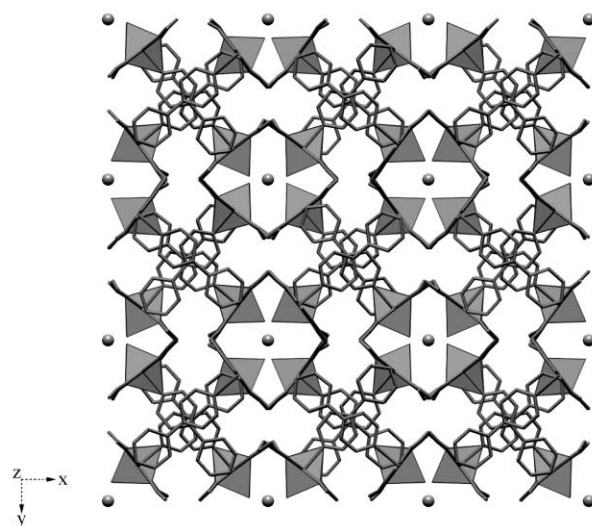
**Fig. 1** ORTEP²¹ view (50% probability) of the asymmetric unit for **1**.**Fig. 2** Extension of the chains along the [001] direction for **1**.

There are three different intermetallic distances between adjacent Fe atoms in this structure: the shortest one (6.50 Å) corresponds to non-bridged atoms but connected to the same four Fe atoms, the intermediate distance (7.90 Å) takes place through Fe atoms linked through N2–C1–N7–C2–N3 dca ligands (the Fe–N7–Fe angle is 119.3°) and the longest one (8.27 Å) is the distance between Fe atoms linked through N4–C3–N6–C4–N5 dca ligands (Fe–N6–Fe average angle is 129.1°).

Table 3 displays the selected bonded parameters for **1**. As observed, the octahedral environment is slightly axially elongated (Fe–O_{water} and Fe–N_{bipy} average distances are respectively 2.22(1) and 2.191(4) Å while Fe–N_{dca} is 2.151(9) Å).

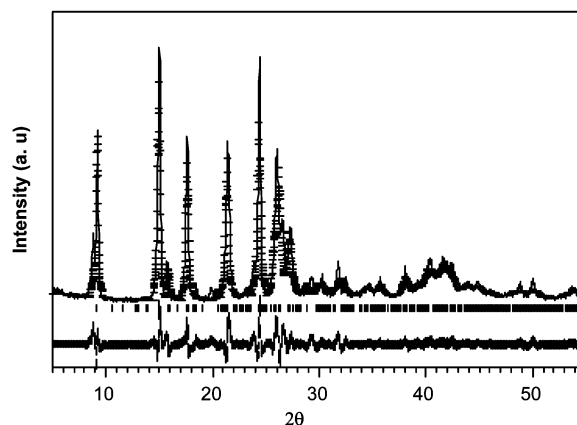
The 1D chains for **1** are packed on *xy* planes as shown in Fig. 3. As observed, consecutive chains are perpendicularly disposed. This way, the bipy ligands are piled parallel to the extension of the chains.

Manson *et al.*¹⁵ have reported an isomorphous Mn compound (**4**). These authors report a crystallographic character-

**Fig. 3** Polyhedral model of the crystal structure for **1** (crystallisation molecules of water have been plotted on ideal positions for clarity).

isation on the basis of a lower symmetry space group (*Iba2*, $a = 22.378(6)$, $b = 22.517(5)$, $c = 13.519(5)$ Å). It should be mentioned that, to the best of our knowledge, isomorphous compounds **1** and **4** are the only examples of monodentate coordinated bipy. As explained below, this fact can be explained by considering the Pearson acidity of the metallic cations.

Compound **2** has been determined to be isomorphous to **3** by means of X-ray powder diffraction pattern analysis. Fig. 4

**Fig. 4** Observed, calculated and difference X-ray diffraction patterns for **2**.

displays the observed, calculated and difference X-ray diffraction pattern for **2** according to the crystallographic data shown in Table 2. As seen, there is a good agreement between theoretical and experimental data.

According to this isomorphism, the structure for **2** consists of two interpenetrated α -Po-type 3D frameworks where the metallic atoms are linked through μ -1,5-dca and N,N'-bipy bridges. Fig. 5 shows a graphical representation of one of the interpenetrated frameworks. As observed, four dca groups are located on the equatorial sites and two bipy ligands are axially coordinated. The equatorial positions of the octahedral coordination are located on the *xz* planes while the axial sites lie on the [010] direction.

The intermetallic distances through dca and bipy bridges for compound **2** should be around 8.5 and 11.5 Å, respectively (similarly to compound **3**). This disposition gives rise to large cavities that account for the occurrence of the interpenetrating frameworks.

As seen in Fig. 6, the metallic atoms of the second framework are located on the centres of these cavities. This way, the

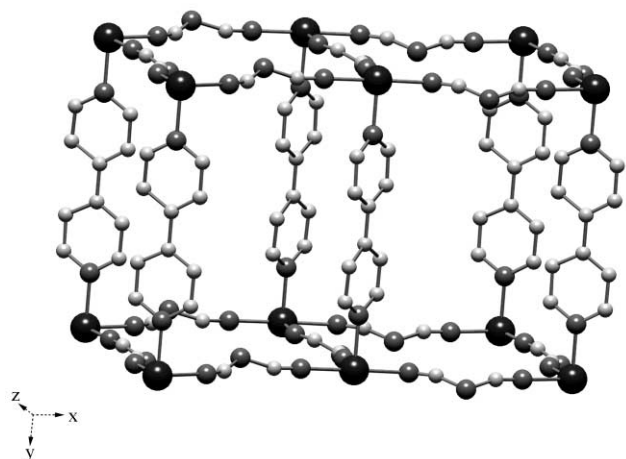


Fig. 5 View of one of the interpenetrated α -Po-type 3D frameworks for **2**.

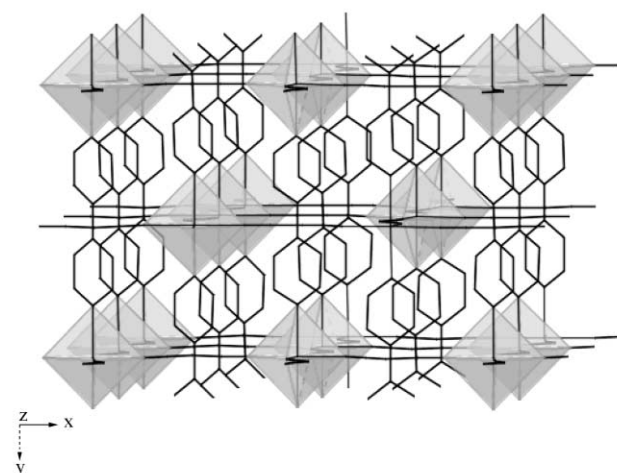


Fig. 6 Representation with a polyhedral model of the crystal structure for **2** showing both interpenetrated α -Po-type 3D frameworks.

shortest intermetallic distance occurs between metallic atoms belonging to different frameworks (intermetallic average distance for **3** is 8.36 Å).

Influence of the nature of the metallic cation

Considering that the synthesis strategy used for **1** and **2** was the same, the two different structures obtained could be explained by the formation, in both cases, of $[M(dca)_2(bipy)(H_2O)_3]$ monomers and their different polymerisation based on the different Pearson-acidities of the Fe^{II} and Ni^{II} cations. A suggestion to explain the different polymerisation is given in Chart 2. The 3D polymerisation of the Ni-monomers for **2** should imply removal of the three molecules of water in the monomeric units (marked as O). This way, a 'cubic' polymerisation can be proposed taking place *via* equatorial attack of the dca groups and axial attack of the bipy ligands. For **1**, however, the bipy ligands cannot remove the axial molecules of water in the monomeric units (marked as H_2O). This difference can be explained by considering the higher Pearson-acidity of Fe^{II} . As a result, the bipy ligands remain monodentate and the geometry of the polymerisation becomes octahedral in order to obtain efficient packing.

On the basis of the decreasing acidity from Mn^{II} to Ni^{II} (which accounts for the decreasing tendency to coordinate to O-donor ligands and the increasing tendency to chelate to N-donors), this hypothesis would also explain the isomorphism between compounds **1** (Fe) and **4** (Mn), on the one hand, and **2** (Ni) and **3** (Co) on the other.

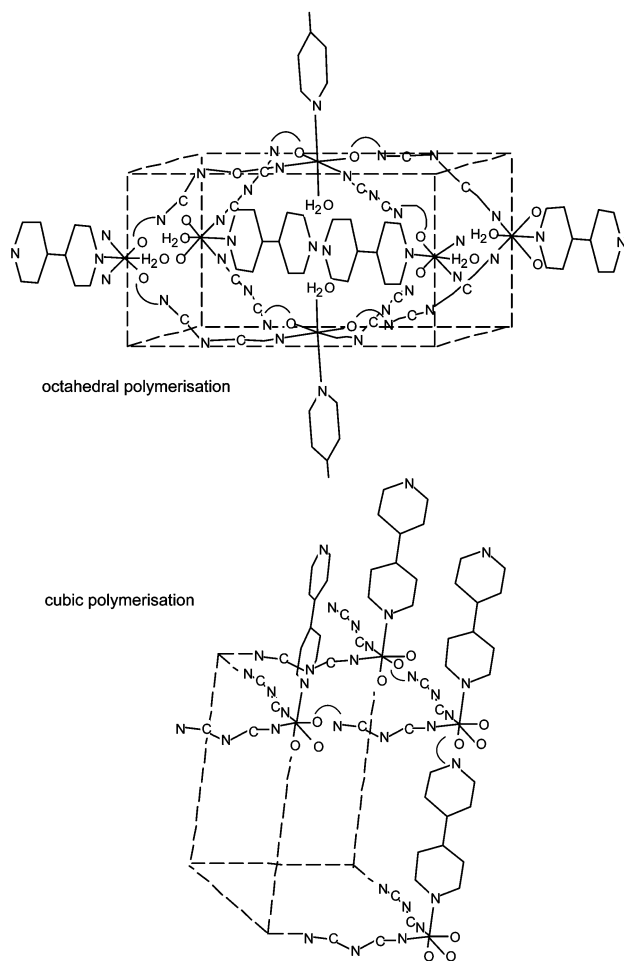


Chart 2

Table 4 IR bands (cm^{-1}) and assignments for compounds **1** and **2**

	1	2
dca, $\nu_{sym} + \nu_{asym} (C\equiv N)$	2325/2295	2312
dca, $\nu_{asym} (C\equiv N)$	2245	2257
dca, $\nu_{sym} (C\equiv N)$	2225/2155	2190
Pyridyl ring stretching	1600/1530	1615/1495
Pyridyl ring breathing	1045	1055
ν_{M-N}	535/520	540/520
H_2O , crystallisation (O–H)	3400m	

IR and UV-Vis spectroscopies

A summary of the most important IR bands corresponding to compounds **1** and **2** together with their tentative assignment¹⁶ is given in Table 4. Both compounds exhibit strong absorptions in the region 2325–2155 cm^{-1} that correspond to $\nu_{C\equiv N}$ modes for dca groups. There are also strong bands at about 1600 cm^{-1} for both compounds (with a shoulder at lower wavenumbers) that have been attributed to the characteristic ring stretching for bipy groups. Additionally, pyridyl ring breathing signals have been detected around 1050 cm^{-1} . Less significant absorptions around 530 cm^{-1} can be assigned to ν_{M-N} modes. Finally, compound **1** shows a broad signal at about 3400 cm^{-1} which corresponds to water.

The UV-Vis diffuse reflectance spectrum for compound **1** reveals two signals, $\nu_1 = 9200$ and $\nu_2 = 11000$ cm^{-1} , which have been attributed to transitions from $^5T_{2g}$ to 5A_1 and 5B_1 states, respectively. Both terms result from the split of the 5E_g term as a consequence of the Jahn–Teller effect. The calculated values of $D_q = 920$ cm^{-1} and $(8/3)d\sigma = 1800$ cm^{-1} are consistent with Fe^{II} ions in an octahedral environment.¹⁷

For compound **2**, the UV-Vis diffuse reflectance spectrum exhibits signals at $\nu_1 = 10100$, $\nu_2 = 16500$ and $\nu_3 = 29500 \text{ cm}^{-1}$ which have been attributed to transitions from ${}^3A_{2g}$ to ${}^3T_{2g}$, ${}^3T_{1g}(F)$, and ${}^3T_{1g}(P)$, respectively. Additionally, a spin forbidden transition from ${}^3A_{2g}$ to 1E_g has been detected at 13500 cm^{-1} . According to this assignment, $D_q = 1010 \text{ cm}^{-1}$, $B = 940 \text{ cm}^{-1}$ and $C = 3525 \text{ cm}^{-1}$ parameters have been calculated that are typical for Ni^{II} ions in an octahedral environment. The value for B represents a 90.3% of the theoretical one for free octahedral Ni^{II} ions.

Magnetic properties

Measurements of the thermal variation of the magnetic susceptibility for compounds **1** and **2** showed that χ_m values continuously increase upon cooling for both compounds, not exhibiting any maxima over the whole studied temperature range.

The experimental data for compound **1**, plotted as the thermal variation of the reciprocal molar susceptibility and the $\chi_m T$ product are shown in Fig. 7. The variation of χ_m^{-1} is well

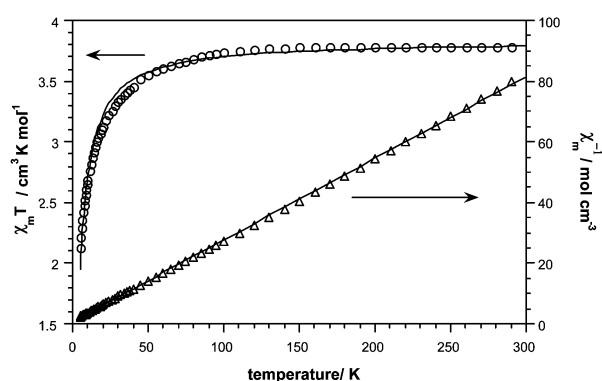


Fig. 7 Thermal evolution of χ_m^{-1} and $\chi_m T$ for **1** and their corresponding theoretical curves (solid lines).

described by the Curie–Weiss law over the whole range of temperature, with values of $C_m = 3.72 \text{ cm}^3 \text{ K mol}^{-1}$ and $\theta = -3.1 \text{ K}$. The $\chi_m T$ term is practically constant down to 100 K ($\chi_m T = 3.78 \text{ cm}^3 \text{ K mol}^{-1}$ at room temperature), rapidly decreasing upon further cooling.

The thermal variation of $\chi_m T$ together with the sign of the Weiss constant could be consistent with the occurrence of antiferromagnetic coupling taking place through the dca groups. In order to evaluate the exchange constant J , eqn. (1) can be proposed as a theoretical approach to the magnetic behaviour of compound **1**. In this expression, χ_m is a function of the J parameter due to exchange coupling along an infinite-spin, linear chain¹⁸ with $S = 2$,

$$\chi_m = \frac{6Ng^2\beta^2}{3kT} \left[\frac{1-u}{1+u} \right] \quad (1)$$

$$\text{where } u = \frac{T}{T_0} - \coth\left(\frac{T}{T_0}\right) \text{ and } T_0 = 12 \frac{J}{K}$$

N and k are the Avogadro and Boltzmann constants, respectively, and β is the Bohr magneton.

According to eqn. (1), the best fit parameters for compound **1** have been determined to be $g = 2.26$ and $J = -0.3 \text{ cm}^{-1}$. The calculated value of g lies among the usual ones for octahedral Fe^{II} (2.08–2.33).¹⁹ The low value of J is consistent with the poor magnetic mediator nature of the dca ligand.

Fig. 8 displays the thermal variation of the reciprocal molar susceptibility and the $\chi_m T$ product for **2**. As observed, the

Curie–Weiss law is followed for the whole range of temperatures studied with values of $C_m = 1.159 \text{ cm}^3 \text{ K mol}^{-1}$ and $\theta = +2.0 \text{ K}$. The $\chi_m T$ product slowly increases from $1.152 \text{ cm}^3 \text{ K mol}^{-1}$ at room temperature to $1.317 \text{ cm}^3 \text{ K mol}^{-1}$ at 12.5 K tending to zero under further cooling.

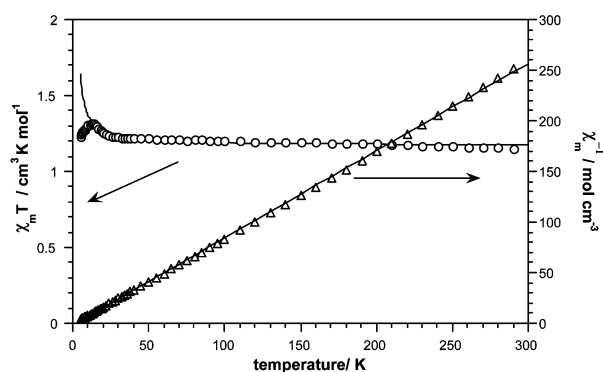


Fig. 8 Thermal evolution of χ_m^{-1} and $\chi_m T$ for **2** and their corresponding theoretical curves (solid lines).

The positive value of θ and the increasing slope of $\chi_m T$ down to 12.5 K are indicative of the occurrence of weak ferromagnetic interactions for compound **2** while the decrease of $\chi_m T$ can be explained by the characteristic zero-field-splitting for Ni^{II} ions.

Since the alignment of the spins of cations bonded through dca and bipy ligands should be antiparallel, the net ferromagnetic component should be attributed to the interaction between both interpenetrated networks. Thus, as shown in Chart 3, consecutive metallic centres along the [102] direction

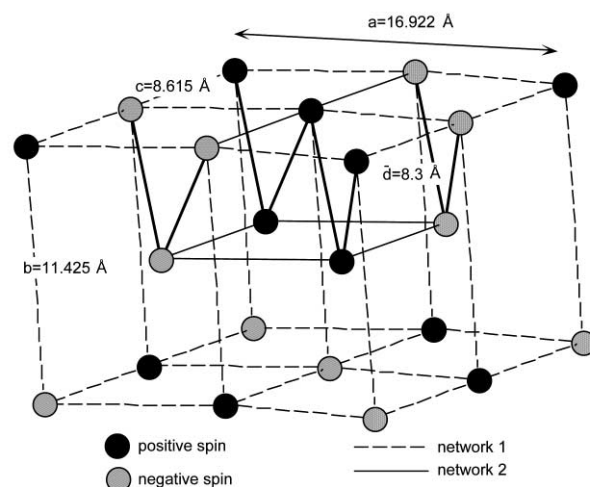


Chart 3

corresponding to networks 1 and 2, must be aligned in parallel. The second possibility (with the spins of metallic centres on network 2 opposite to those in Chart 3) would correspond to the same situation along the $[-102]$ direction. This way, for the net interaction to be ferromagnetic, parallel coupling between atoms of different networks should be more important than the one corresponding to the antiparallel exchange between atoms of the same network. It is worth noting that the intermetallic distance between atoms belonging to different networks is the shortest in this structure (8.3 Å on average).

According to the above, a 1D parallel magnetic coupling should be responsible for the increasing $\chi_m T$ upon cooling for **2**. In order to estimate this net ferromagnetic exchange, eqn. (2) has been used in which χ_m is a function of the J parameter due to exchange coupling along an infinite-spin, linear chain²⁰ with $S = 1$.

$$\chi_m = \frac{Ng^2\beta^2}{kT} \left(\frac{2 - 0.0194\frac{x}{T} + 0.777\left(\frac{x}{T}\right)^2}{3 - 4.346\frac{x}{T} + 3.232\left(\frac{x}{T}\right)^2 - 5.834\left(\frac{x}{T}\right)^3} \right) \quad (2)$$

where $x = \frac{J}{k}$

N and k are the Avogadro and Boltzmann constants, respectively, and β is the Bohr magneton.

As observed in Fig. 8, eqn. (2) reproduces the increasing $\chi_m T$ quite well with values of $J = 1.05 \text{ cm}^{-1}$ and $g = 2.16$. The estimated value of J is consistent with the weak character of the coupling while the value of g lies among the usual ones for octahedral Ni^{II} .¹⁹

Concluding remarks

The compounds reported in this paper illustrate the influence of the nature of the metallic cation on the structural features of M^{II} -dca-bipy ($\text{M} = \text{Fe}, \text{Ni}$) extended systems. Even if for both of them each metallic cation is connected to another four through μ -1,5-dca bridges, the distinct performance of the bipy ligands results in different structural features and connectivity which accounts for their distinct magnetic behaviour.

Acknowledgements

This work has been carried out with the financial support of the Universidad del País Vasco/Euskal Herriko Unibertsitatea (Grant 9/UPV 00169.125-13956/2001), and the Gobierno Vasco/Eusko Jaurlaritz (Grant PI99/53). S. M. also thanks the Gobierno Vasco for the doctoral fellowship associated to the project PI96/39.

References

- (a) S. R. Batten, P. Jensen, B. Moubaraki, K. S. Murray and R. Robson, *Chem. Commun.*, 1998, 439; (b) J. L. Manson, D. W. Lee, A. L. Rheingold and J. S. Miller, *Inorg. Chem.*, 1998, **37**, 5966; (c) J. L. Manson, C. R. Kmety, A. J. Epstein and J. S. Miller, *Inorg. Chem.*, 1999, **38**, 2552; (d) P. Jensen, S. R. Batten, G. D. Fallon, B. Moubaraki, K. S. Murray and D. J. Price, *Chem. Commun.*, 1999, 177; (e) S. R. Batten, P. Jensen, C. J. Kepert, M. Kurmoo, B. Moubaraki, K. S. Murray and D. J. Price, *J. Chem. Soc., Dalton Trans.*, 1999, 2987; (f) P. Jensen, S. R. Batten, G. D. Fallon, D. C. R. Hockless, B. Moubaraki, K. S. Murray and R. Robson, *J. Solid State Chem.*, 1999, **145**, 387; (g) J. L. Manson, A. M. Arif and J. S. Miller, *J. Mater. Chem.*, 1999, **9**, 979; (h) P. Jensen, S. R. Batten, B. Moubaraki and K. S. Murray, *Chem. Commun.*, 2000, 793; (i) A. Escuer, F. A. Mautner, N. Sanz and R. Vicente, *Inorg. Chem.*, 2000, **39**, 1668; (j) S. R. Batten, A. R. Harris, P. Jensen, K. S. Murray and A. Ziebell, *J. Chem. Soc., Dalton Trans.*, 2000, 3829; (k) J. Kohout, L. Jager, M. Hvastijová and J. Kozisek, *J. Coord. Chem.*, 2000, **51**, 169; (l) I. Dasna, S. Golhen, L. Ouahab, N. Daro and J.-P. Sutter, *New J. Chem.*, 2001, **25**, 1572; (m) P. Jensen, S. R. Batten, B. Moubaraki and K. S. Murray, *J. Solid State Chem.*, 2001, **159**, 352; (n) N. Moliner, A. B. Gaspar, M. C. Muñoz, V. Niel, J. Cano and J. A. Real, *Inorg. Chem.*, 2001, **40**, 3986; (o) P. M. van der Werf, S. R. Batten, P. Jensen, B. Moubaraki and K. S. Murray, *Inorg. Chem.*, 2001, **40**, 1718; (p) R. Clerac, F. A. Cotton, S. P. Jeffery, C. A. Murillo and X. Wang, *Inorg. Chem.*, 2001, **40**, 1265; (q) B. Vangdal, J. Carranza, F. Lloret, M. Julve and J. Sletten, *J. Chem. Soc., Dalton Trans.*, 2002, 566.
- (a) I. Potocnák, M. Dunaj-Jurco, D. Miklos and L. Jäger, *Acta Crystallogr., Sect. C*, 1996, **52**, 1653; (b) I. Potocnák, M. Dunaj-Jurco, D. Miklos and M. Kabesová, *Acta Crystallogr., Sect. C*, 1995, **51**, 600.
- (a) Y. M. Chow, *Inorg. Chem.*, 1971, **10**, 1938; (b) Y. M. Chow and D. Britton, *Acta Crystallogr., Sect. C*, 1977, **33**, 697; (c) D. Britton, *Acta Crystallogr., Sect. C*, 1990, **46**, 2297; (d) J. L. Manson, C. D. Incarvito, A. L. Rheingold and J. S. Miller, *J. Chem. Soc., Dalton Trans.*, 1998, 3705; (e) J. Mrozinski, M. Hvastijová and J. Kohout, *Polyhedron*, 1992, **11**, 2867.
- J. L. Manson, C. R. Kmety, Q. Huang, J. W. Lynn, G. Bendele, S. Pagola, P. W. Stephens, L. M. Liable-Sands, A. L. Rheingold, A. J. Epstein and J. S. Miller, *Chem. Mater.*, 1998, **10**, 2552.
- Y. M. Chow and D. Britton, *Acta Crystallogr., Sect. C*, 1975, **31**, 1934.
- (a) S. Martin, M. G. Barandika, R. Cortes, J. I. R. Larramendi, M. K. Urriaga, L. Lezama, M. I. Arriortua and T. Rojo, *Eur. J. Inorg. Chem.*, 2001, 2107; (b) S. Martin, M. G. Barandika, J. I. R. Ruiz Larramendi, R. Cortes, M. Font-Bardia, L. Lezama, Z. E. Serna, X. Solans and T. Rojo, *Inorg. Chem.*, 2001, **40**, 3687.
- S. R. Marshall, C. D. Incarvito, J. L. Manson, A. L. Rheingold and J. S. Miller, *Inorg. Chem.*, 2000, **39**, 1969. These authors reported the low temperature structure for $[\text{Co}(\text{dca})_2\text{bpm}]\cdot\text{H}_2\text{O}$.
- (a) M. Kondo, T. Yoshitomi, K. Seki, H. Matsuzaka and S. Kitagawa, *Angew. Chem., Int. Ed. Engl.*, 1997, **36**, 1725; (b) J. Lu, T. Paliwala, S. C. Lim, C. Yu, T. Niu and A. J. Jacobson, *Inorg. Chem.*, 1997, **36**, 923; (c) M.-L. Tong, X.-M. Chen, X.-L. Yu and T. C. W. Mak, *J. Chem. Soc., Dalton Trans.*, 1998, 5; (d) M.-L. Tong, B.-H. Ye, J.-W. Cai, X.-M. S. W. Chen and Ng, *Inorg. Chem.*, 1998, **37**, 2645; (e) J. Y. Lu, B. R. Cabrera, R.-J. Wang and J. Li, *Inorg. Chem.*, 1999, **38**, 4608; (f) J. Y. Lu, M. A. Lawandy, J. Li, T. Yuen and C. L. Lin, *Inorg. Chem.*, 1999, **38**, 2695; (g) K. Biradha, K. V. Domasevitch, B. Moulton, C. Seward and M. J. Zawarotko, *Chem. Commun.*, 1999, 1327; (h) L.-M. Zheng, X. Fang, K.-H. Lii, H.-H. Song, X.-Q. Xin, H.-K. Fun, K. Chinnakali and I. A. Razak, *J. Chem. Soc., Dalton Trans.*, 1999, 2311; (i) S. Han, J. L. Manson, J. Kim and J. S. Miller, *Inorg. Chem.*, 2000, **39**, 4182; (j) Z. Shi, S. Feng, S. Gao, L. Zhang, G. Yang and J. Hua, *Angew. Chem., Int. Ed.*, 2000, **39**, 2325; (k) S. Han, J. L. Manson, J. Kim and J. S. Miller, *Inorg. Chem.*, 2000, **39**, 4182; (l) Z. Shi, S. Feng, S. Gao, L. Zhang, G. Yang and J. Hua, *Angew. Chem., Int. Ed.*, 2000, **39**, 2325; (m) Y.-C. Jiang, Y.-C. Lai, S.-L. Wang and K.-H. Lii, *Inorg. Chem.*, 2001, **40**, 5320; (n) Z. Shi, S. Feng, Y. Sun and J. Hua, *Inorg. Chem.*, 2001, **40**, 5312; (o) S. Martin, M. G. Barandika, L. Lezama, J. L. Pizarro, Z. E. Serna, J. I. R. Larramendi, M. I. Arriortua, T. Rojo and R. Cortes, *Inorg. Chem.*, 2001, **40**, 4109; (p) E. Suresh, K. Boopalan, R. V. Jasra and M. M. Bhadbhade, *Inorg. Chem.*, 2001, **40**, 4078; (q) Q.-F. Zhang, Y. Niu, X. Xin, W.-H. Leung, I. D. Williams and Y. Song, *Chem. Commun.*, 2001, 1126.
- A. Altomare, G. Cascarano, C. Giacovazzo, A. Guagliardi, A. G. G. Moliterni, M. C. Burla, G. Polidori, M. Camalli, R. A. Spagna, Package for Crystal Structure Solution by Direct Methods and Refinement, Universities of Bari, Perugia and Roma, Italy, 1997.
- G. M. Sheldrick, SHELXL97, Program for the Refinement of Crystal Structures, University of Göttingen, Germany, 1997.
- International Tables for X-Ray Crystallography*, vol. IV, Kynoch Press, Birmingham, UK, 1974.
- J. Rodriguez-Carvajal, FULLPROF, Program Rietveld Pattern Matching Analysis of Powder Patterns, 1997.
- (a) H. M. Rietveld, *Acta Crystallogr.*, 1967, **12**, 151; (b) H. M. Rietveld, *J. Appl. Crystallogr.*, 1969, **6**, 65.
- B.-W. Sun, S. Gao, B.-Q. Ma and Z.-M. Wang, *New J. Chem.*, 2000, **24**, 953.
- (a) J. L. Manson, A. M. Arif, C. D. Incarvito, L. M. Liable-Sands, A. L. Rheingold and J. S. Miller, *J. Solid State Chem.*, 1999, **145**, 369; (b) J. L. Manson, C. D. Incarvito, A. M. Arif, A. L. Rheingold and J. S. Miller, *Mol. Cryst. Liq. Cryst.*, 1999, **334**, 605.
- K. Nakamoto, *Infrared Spectra of Inorganic and Coordination Compounds*, John Wiley & Sons, New York, 1997.
- A. B. P. Lever, *Inorganic Electronic Spectroscopy*, Elsevier, London, 1984.
- M. E. Fisher, *Am. J. Phys.*, 1964, **32**, 343.
- F. E. Mabbs and D. J. Machin, *Magnetism and Transition Metal Complexes*, Chapman and Hall, London, 1973.
- G. S. Rushbrook and P. J. Wood, *Mol. Phys.*, 1963, **6**, 409.
- M. N. Burnett and C. K. Johnson, ORTEP3, Report ORNL-6895, Oak Ridge National Laboratory, Oak Ridge, TN, 1996.